Adsorption-Induced Conformational Changes in Fibronectin Due to Interactions with Well-Defined Surface Chemistries

Kristin E. Michael,[†,‡] Varadraj N. Vernekar,[§] Benjamin G. Keselowsky,[‡,||] J. Carson Meredith,[⊥] Robert A. Latour,[§] and Andrés J. García*[,†,‡]

Woodruff School of Mechanical Engineering, Georgia Institute of Technology, Atlanta, Georgia 30332, Petit Institute for Bioengineering and Bioscience, Georgia Institute of Technology, Atlanta, Georgia 30332, Department of Bioengineering, Clemson University, Clemson, South Carolina 29634, Coulter School of Biomedical Engineering, Georgia Institute of Technology, Atlanta, Georgia 30332, and School of Chemical Engineering, Georgia Institute of Technology, Atlanta, Georgia 30332

Received May 12, 2003. In Final Form: June 30, 2003

Protein adsorption onto synthetic materials influences cell adhesion and signaling events that direct cell function in numerous biomedical applications. Adsorption of fibronectin (FN) to different surfaces alters protein structure and modulates $\alpha_5\beta_1$ integrin binding, cell adhesion, cell spreading, and cell migration. In the present study, self-assembled monolayers of alkanethiols on Au were used to analyze the effects of surface chemistry (CH_3, OH, NH_2, and COOH) on the adsorption of a recombinant fragment of FN, $FNIII_{7-10}$, that incorporates both the synergy and RGD cell binding motifs. Surface chemistry potentiated differential $FNIII_{7-10}$ adsorption kinetics and adsorbed structure as determined by surface plasmon resonance spectroscopy and antibody binding assays. $FNIII_{7-10}$ functional activity, determined by cell adhesion strength, was modulated in a fashion consistent with these structural changes ($OH = NH_2 > COOH > CH_3$). However, these changes in protein parameters did not correlate simply to differences in surface hydrophobicity, indicating that additional surface parameters influence protein adsorption. These results demonstrate that surface chemistry modulates adsorbed protein structure and activity and establish a relationship between surface-dependent changes in structural domains of $FNIII_{7-10}$ and functional activity.

Introduction

Protein adsorption plays a critical role in numerous biomedical and biotechnological applications. Adsorption of proteins onto synthetic surfaces is a thermodynamically driven process.[1] Due to the diverse circumstances in which proteins and surfaces come in contact, an understanding of protein adsorption is fundamental to fields as varied as bioseparation, development of biosensors, food processing, and implant technology.[1,2] In addition to activating blood clotting and inflammatory responses, adsorbed proteins mediate cell adhesion to synthetic surfaces. Cell adhesion to adsorbed proteins is particularly important in cell function, host responses to implants, and design of tissue engineering substrates.[3−5]

Protein adsorption is a complex, dynamic process involving noncovalent interactions, including hydrophobic interactions, electrostatic forces, hydrogen bonding, and van der Waals forces.[1] Protein parameters including primary structure, size, and structural stability as well as surface properties such as surface energy, roughness, and chemistry have been identified as key factors influencing the adsorption process.[6−9] In particular, surface chemistry influences adsorbed protein type, quantity, and conformation.[10−12] For example, adsorption of the extracellular matrix protein fibronectin (FN) on different surfaces alters protein structure and modulates cell adhesion, spreading, and migration.[13−16] Although these adsorption studies provide insights into the relationship

* Corresponding author. Address: Woodruff School of Mechanical Engineering, 315 Ferst Drive, Room 2314 IBB, Atlanta, GA 30332-0363. E-mail: andres.garcia@me.gatech.edu. Phone: 404-894-9384. Fax: 404-385-1397.

† Woodruff School of Mechanical Engineering, Georgia Institute of Technology.

‡ Petit Institute for Bioengineering and Bioscience, Georgia Institute of Technology.

§ Department of Bioengineering, Clemson University.

|| Coulter School of Biomedical Engineering, Georgia Institute of Technology.

⊥ School of Chemical Engineering, Georgia Institute of Technology.

(1) Andrade, J. D.; Hlady, V. *Adv. Polym. Sci.* **1986**, *79*, 1−63.

(2) Brash, J. L.; Horbett, T. A. In *Proteins at Interfaces II*: *Fundamentals and Applications*; Horbett, T. A., Brash, J. L., Eds.; ACS Symposium Series No. 602; American Chemical Society: Washington, DC, 1995; pp 1−25.

(3) Park, P. K.; Jarrell, B. E.; Williams, S. K.; Carter, T. L.; Rose, D. G.; Martinez-Hernandez, A.; Carabasi, R. A., III *J. Vasc. Surg.* **1990**, *11*, 468−475.

(4) Anderson, J. M. *ASAIO Trans.* **1988**, *34*, 101−107.

(5) Langer, R.; Vacanti, J. P. *Science* **1993**, *260*, 920−926.

(6) Brash, J. L. In *Proteins at Interfaces*: *Physicochemical and Biochemical Studies*; Brash, J. L., Horbett, T. A., Eds.; ACS Symposium Series No. 343; American Chemical Society: Washington, DC, 1987; pp 490−506.

(7) Haynes, C. A.; Sliwinsky, E.; Norde, W. *J. Colloid Interface Sci.* **1994**, *164*, 394−409.

(8) Deligianni, D. D.; Katsala, N.; Ladas, S.; Sotiropoulou, D.; Amedee, J.; Missirlis, Y. F. *Biomaterials* **2001**, *22*, 1241−1251.

(9) Denis, F. A.; Hanarp, P.; Sutherland, D. S.; Gold, J.; Mustin, C.; Rouxhet, P. G.; Dufrene, Y. F. *Langmuir* **2002**, *18*, 819−828.

(10) Prime, K. L.; Whitesides, G. M. *Science* **1991**, *252*, 1164−1167.

(11) Shen, M.; Horbett, T. A. *J. Biomed. Mater. Res.* **2001**, *57*, 336−345.

(12) Tengvall, P.; Lundstrom, I.; Liedberg, B. *Biomaterials* **1998**, *19*, 407−422.

(13) Grinnell, F.; Feld, M. K. *J. Biomed. Mater. Res.* **1981**, *15*, 363−381.

(14) Iuliano, D. J.; Saavedra, S. S.; Truskey, G. A. *J. Biomed. Mater. Res.* **1993**, *27*, 1103−1113.

(15) Pettit, D. K.; Hoffman, A. S.; Horbett, T. A. *J. Biomed. Mater. Res.* **1994**, *28*, 685−691.

(16) Garcia, A. J.; Vega, M. D.; Boettiger, D. *Mol. Biol. Cell* **1999**, *10*, 785−798.

10.1021/la034810a CCC: $25.00
Published on Web 08/02/2003

between surface properties and protein adsorption, many of these experimental systems lack surface homogeneity or have indeterminable surface properties. Recent studies have focused on using model surfaces, such as self-assembled monolayers (SAMs) of alkanethiols on Au, that allow the systematic investigation of the effects of surface chemistry on protein adsorption without altering other surface properties.[10,17−20]

Current models for protein adsorption indicate that the adsorption process induces a partial unfolding of protein as determined by Fourier transform infrared (FTIR) spectroscopy, NMR, atomic force microscopy (AFM), and total internal reflectance fluorescence (TIRF) spectroscopy.[21−28] For example, Raghavachari et al. recently observed structural rearrangements within the repeat units of von Willebrand factor multimers upon adsorption to hydrophobic supports.[28] Similarly, Wertz and Santore demonstrated a change in protein footprint area during adsorption due to a partial unfolding or reorientation of the protein, and the rate of this conformational change was dependent on surface hydrophobicity.[24−27] Although these studies document changes in protein structure/conformation, the only surface characteristic studied was surface hydrophobicity and the effects of the adsorption-induced structural alterations on protein activity remain poorly understood. Protein activity is a crucial consideration as modulation in activity can regulate higher order cell functions.[16] Therefore, protein activity is another important parameter for analyzing protein adsorption.

We previously demonstrated that upon adsorption onto alkanethiol SAMs presenting different chemistries, FN undergoes changes in structure that modulate $\alpha_5\beta_1$ integrin binding and cell adhesion.[29] The objective of the present study was to analyze adsorption-induced conformational changes in the central cell binding region of FN as a function of surface chemistry. A recombinant fragment of FN ($FNIII_{7-10}$) that incorporates both the PHSRN synergy and RGD binding motifs was used to model the full plasma FN molecule and isolate the central cell binding domain. SAMs of alkanethiols on Au presenting hydrophobic (CH_3), neutral hydrophilic (OH), positively charged (NH_2), and negatively charged (COOH) surfaces were used to examine the effects of surface chemistry on $FNIII_{7-10}$ adsorption. Using kinetic and quasi-equilibrium assays, we demonstrate significant surface-chemistry-dependent structural changes in FN binding domains and adhesive activity. These findings establish a relationship between surface-dependent changes in structural domains of FN and functional activity.

Materials and Methods

Reagents. LB agar, LB broth, ampicillin, and IPTG used for bacteria culture and protein production were obtained from Invitrogen (Carlsbad, CA). Chemical reagents, CellLytic B-Clear II, and DNAse I used for bacteria lysis and $FNIII_{7-10}$ purification were obtained from Sigma Chemical (St. Louis, MO). HiTrap Q Sepharose Fast Flow anion exchange chromatography columns were obtained from Amersham Pharmacia (Piscataway, NJ). Centrifugal concentration devices were purchased from Gelman Laboratory (Ann Arbor, MI), and Slide-A-Lyzer dialysis cassettes used in protein purification were purchased from Pierce Chemical Co. (Rockford, IL). Bolton-Hunter Reagent for $FNIII_{7-10}$ iodination was purchased from NEN Life Science Products (Boston, MA), and Calcein-AM used in cell adhesion detection was acquired from Molecular Probes (Eugene, OR). Cell culture reagents, DPBS, PBS without Ca^{2+} or Mg^{2+}, and human plasma fibronectin (pFN) were purchased from Invitrogen. Newborn calf serum was obtained from Hyclone (Logan, UT).

Antibodies and Cells. Several antibodies (Ab's) were used as structural probes for adsorbed FN in enzyme-linked immunosorbent assays (ELISA). Primary monoclonal Ab HFN7.1 (Developmental Hybridoma, Inc., Iowa City, IA) directed against the flexible linker between the 9th and 10th type III repeat, FnI-11 directed against the 9th type III repeat, and mAb1937 (Chemicon, Temecula, CA) directed against the 8th type III repeat were used.[30,45,46] An alkaline phosphatase-conjugated donkey anti-mouse IgG Ab (Jackson Immunoresearch, West Grove, PA) was used as a secondary Ab against all three primary antibodies. Murine NIH3T3 fibroblasts (CRL-1658, ATCC, Manassas, VA) were grown in Dulbecco's modified Eagle's medium (DMEM) supplemented with 10% newborn calf serum and 1% penicillin/streptomycin.

Surface Preparation and Characterization. SAM surfaces were prepared and characterized as previously described.[29] Alkanethiols 1-dodecanethiol ($HS-(CH_2)_{11}-CH_3$), 11-mercapto-1-undecanol ($HS-(CH_2)_{11}-OH$), and 11-mercaptoundecanoic acid ($HS-(CH_2)_{10}-COOH$) were purchased from Aldrich Chemical (Milwaukee, WI) and used as received. The amine-terminated alkanethiol 12-amino-1-mercaptododecane ($HS-(CH_2)_{12}-N_2H$) was synthesized and characterized by our group.[29] The assembled SAMs of their respective alkanethiols are referred to hereafter as CH_3, OH, COOH, and NH_2.

SAMs were assembled on Au-coated glass chamber slides (16-well Lab-Tek Chamber Slides, Nalge Nunc International, Naperville, IL) for equilibrium conformation and cell adhesion studies. Au-coated glass coverslips (9 mm square, Belco Glass, Inc., Vineland, NJ) were used as SAM substrates for radiolabeling and kinetic adsorption experiments. Glass chamber slides were cleaned by O_2 plasma etching in a Plasma Preen II-862 Plasma Cleaner (Plasmatic Systems, Inc., North Brunswick, NJ), and coverslips were cleaned with 70% H_2SO_4 and 30% H_2O_2 at 90 °C for 1 h, rinsed with deionized H_2O (diH_2O), rinsed with 95% ethanol, and dried under a stream of N_2 prior to metal deposition. Au-coated substrates were prepared by deposition of thin films of Ti (150 Å) followed by Au (150 Å) using an electron beam evaporator (Thermionics Laboratories, Hayward, CA) at a deposition rate of 2 Å/s and a chamber base-pressure of approximately 2×10^{-6} Torr.

Freshly prepared Au surfaces were immersed in alkanethiol solutions (1 mM in absolute ethanol), and SAMs were allowed to assemble overnight (16 h). SAMs were rinsed in 95% ethanol, dried under N_2, and allowed to equilibrate in DPBS for 15 min prior to incubation in $FNIII_{7-10}$ solutions. Surfaces were validated by contact angle measurements. Ambient air−water−substrate contact angle measurements (5 μL of deionized H_2O) were taken with a Rame-Hart model no. 100-00 goniometer (Mountain Lakes, NJ) fitted with a digital camera and analyzed using in-house image analysis software.

(17) Tegoulia, V. A.; Cooper, S. L. *J. Biomed. Mater. Res.* **2000**, *50*, 291−301.
(18) Singhvi, R.; Kumar, A.; Lopez, G. P.; Stephanopoulos, G. N.; Wang, D. I.; Whitesides, G. M.; Ingber, D. E. *Science* **1994**, *264*, 696−698.
(19) Franco, M.; Nealey, P. F.; Campbell, S.; Teixeira, A. I.; Murphy, C. J. *J. Biomed. Mater. Res.* **2000**, *52*, 261−269.
(20) Tidwell, C. D.; Ertel, S. I.; Ratner, B. D. *Langmuir* **1997**, *13*, 3404−3413.
(21) Buijs, J.; Norde, W.; Lichtenbelt, J. W. T. *Langmuir* **1996**, *12*, 1605−1613.
(22) Danielson, M. A.; Falke, J. J. *Annu. Rev. Biophys. Biomol. Struct.* **1996**, *25:163−95*, 163−195.
(23) Xia, N.; May, C. J.; McArthur, S. L.; Castner, D. G. *Langmuir* **2002**, *18*, 4090−4097.
(24) Norde, W.; Haynes, C. A. In *Proteins at Interfaces II*: *Fundamentals and Applications*; Horbett, T. A., Brash, J. L., Eds.; ACS Symposium Series No. 602; American Chemical Society: Washington, DC, 1995; pp 26−40.
(25) Wertz, C. F.; Santore, M. M. *Langmuir* **1999**, *15*, 8884−8894.
(26) Wertz, C. F.; Santore, M. M. *Langmuir* **2001**, *17*, 3006−3016.
(27) Wertz, C. F.; Santore, M. M. *Langmuir* **2002**, *18*, 706−715.
(28) Raghavachari, M.; Tsai, H. M.; Kottke-Marchant, K.; Marchant, R. E. *Colloids Surf., B* **2000**, *19*, 315−324.
(29) Keselowsky, B. G.; Collard, D. M.; Garcia, A. J. *J. Biomed. Mater. Res.* **2003**, *66A*, 247−259.
(30) Schoen, R. C.; Bentley, K. L.; Klebe, R. J. *Hybridoma* **1982**, *1*, 99−108.

Recombinant Fibronectin Fragment. $FNIII_{7-10}$ was produced and purified as described previously.[31] *Escherichia coli* transformed with cDNA coding for human $FNIII_{7-10}$ and ampicillin resistance were streaked onto an LB agar plate containing 100 μg/mL ampicillin and incubated overnight at 37 °C. A single colony was isolated and expanded in 5 mL of LB broth with 50 μg/mL ampicillin for 3−5 h at 37 °C. This starter culture was added to 500 mL of LB + 50 μg/mL ampicillin + 0.4 mM IPTG to induce $FNIII_{7-10}$ expression. The culture was grown overnight at 28 °C. Bacteria pellets were collected at 25 000*g* for 10 min and frozen at −80 °C. Upon thawing, bacteria were lysed and cytosolic proteins were exposed by addition of CellLytic B-Clear II (5 mL/g) and DNAse I (5 μg/mL) for 30 min. The lysate was centrifuged at 25 000*g* for 15 min. Proteins were precipitated by centrifugation in 40% ammonium sulfate for 25 min at 25 000*g*. The pellet was resuspended in 15 mL of start buffer (0.2 M Tris, pH 8.0) and purified by anion exchange chromatography using a BioRad Econo Gradient Pump, UV monitor, and fraction collector (Hercules, CA) with 5 mL HiTrap Q columns. Proteins were bound to the columns, washed with 5 column volumes of start buffer, and eluted via salt gradient (0.2−0.4 M NaCl in 0.5 M Tris, pH 7.7) by stepping up the concentration every 2 column volumes. The desired protein product eluted at approximately 0.27 M NaCl and was verified to be >95% pure $FNIII_{7-10}$ by SDS-PAGE. Relevant fractions were concentrated using Microsep 10K Omega centrifugal devices, dialyzed overnight against CAPS buffer (10 mM CAPS, 150 mM NaCl, pH 11.0), and flash frozen for storage at −80 °C.

Surface Plasmon Resonance Spectroscopy. Protein adsorption kinetics was quantified via surface plasmon resonance (SPR) spectroscopy using a Biacore X instrument (Biacore, Inc., Piscataway, NJ). SAMs assembled on Au-coated 9 mm square coverslips were rinsed with ethanol, rinsed with diH_2O, dried with N_2, and assembled onto a Biacore chip holder (Biacore SIA Au kit, BR-1004-05). The chip was primed twice and equilibrated in the Biacore X by flowing DPBS at 5 mL/min for 3 min. A cleaning injection of 70 μL of detergent (0.3% Triton X-100 in 0.1 M glycine, pH 12) was followed by a rinse with DPBS for 2 min. DPBS (50 μL) was injected into the flow channel (50 μL/min) and recorded for comparison to protein injection. $FNIII_{7-10}$ (50 μL, 10 μg/mL) in DPBS was added at 50 μL/min, and the adsorption profile was recorded. The desorption profile was recorded for 30 s by flowing pure DPBS following the $FNIII_{7-10}$ injection.

Characteristic adsorption parameters based on a mass action adsorption model were obtained by simultaneously solving the governing differential equations and fitting the SPR profile numerically. The solutions were obtained using Matlab 5.0 (Mathworks, Inc., Natick, MA) ordinary differential equation solver (ode45) and a Nelder-Mead least-squares regression analysis. Several initial values were input to the solver to ensure that the fitted parameters were at a global minimum.

$FNIII_{7-10}$ Radiolabeling and Adsorption Measurements. $FNIII_{7-10}$ adsorption onto SAMs was quantified as a function of coating concentration using $^{125}I-FNIII_{7-10}$. $FNIII_{7-10}$ was iodinated with the Bolton-Hunter Reagent as described previously.[16,32] Briefly, the Bolton-Hunter Reagent benzene solvent was evaporated with a gentle stream of N_2, and 100 μg of $FNIII_{7-10}$ (10 μg/μL in 0.1 M sodium borate buffer, pH 8.5) was added and incubated overnight at 4 °C. The coupling reaction was quenched with 50 μL of 0.2 M glycine in 0.1 M sodium borate (pH 8.5). Labeled $FNIII_{7-10}$ ($^{125}I-FNIII_{7-10}$) was purified by size exclusion chromatography in a Sephadex G-25 column. The column was blocked in 1% heat-denatured bovine serum albumin (hd-BSA) overnight prior to use. BSA was denatured by heating at 56 °C for 30 min. Fractions containing $^{125}I-FNIII_{7-10}$ were combined and stored at 4 °C. The specific activity (4.39×10^7 cpm/μg) of $^{125}I-FNIII_{7-10}$ was determined using a COBRA II Auto Gamma counter (Packard Bioscience, Meridien, CT) and the NanoOrange Protein Quantification Kit (Molecular Probes). To ensure that labeling of the protein did not alter adsorption behavior, radiolabeled protein was mixed with nonlabeled protein at various ratios, and adsorption measurements yielded equivalent results for all dilutions. For adsorption measurements, SAMs were incubated for 30 min in a mixture of $^{125}I-FNIII_{7-10}$ and $FNIII_{7-10}$ (1−20 μg/mL coating concentration at 22 °C). Surfaces were then blocked for 30 min in 1% hd-BSA to be consistent with the Ab assays and cell adhesion assays that require blocking of the remaining surface not covered by FN. Hd-BSA was used to block nonspecific interactions such as antibody adsorption to these surfaces ensuring detection of the desired specific interaction. Adsorbed $^{125}I-FNIII_{7-10}$ was quantified, and radioactive counts were converted to adsorbed surface densities (ng/cm^2).

Ab Assay for $FNIII_{7-10}$ Conformation. SAMs were incubated in 2-fold serial dilutions of $FNIII_{7-10}$. Surfaces were then blocked against nonspecific Ab binding using blocking buffer (0.25% hd-BSA, 0.00125% NaN_3, 0.1 M EDTA, 2.5% Tween-20 in PBS) for 1 h at 37 °C. Substrates were incubated in primary Ab (1:4000 for HFN7.1 and mAb1937, 1:10000 for FNI-11 in blocking buffer) for 1 h at 37 °C. After washing and blocking for 10 min, substrates were incubated in alkaline phosphatase-conjugated anti-mouse IgG (1:1000) for 1 h at 37 °C, washed, blocked, and incubated in 4-methylumbelliferyl phosphate (60 μg/mL in 10 mM diethanolamine, pH 9.5) for 45 min at 37 °C. Reaction products were quantified using an HTS 7000 Plus fluorescence plate reader (Perkin-Elmer, Foster City, CA) at 360 nm excitation/465 nm emission.

Cell Adhesion Assay. Cell adhesion to $FNIII_{7-10}$-coated SAMs was measured using a centrifugation assay that applies well-controlled detachment forces.[29,33] SAMs were coated with a range of $FNIII_{7-10}$ concentrations (0−20 μg/mL) for 30 min and blocked in 1% hd-BSA plus 0.1% nonfat dry milk for 30 min to prevent nonspecific adhesion to the substrate. NIH3T3 cells were labeled with 2 μg/mL Calcein-AM and seeded at 200 cells/mm^2 in 2 mM dextrose-DPBS into reassembled chamber slides for 30 min at 22 °C. The 30 min time point was chosen to investigate initial adhesion and reduce any confounding effects of cell spreading or cellular matrix secretion. The initial fluorescence intensity was measured to quantify the number of adherent cells prior to application of centrifugal force. After the wells were filled with media and sealed with transparent adhesive tape, substrates were inverted and spun at a fixed speed in a centrifuge (Beckman Allegra 6, GH 3.8 rotor) to apply a centrifugal force corresponding to 22.4*g*. After centrifugation, media were exchanged and fluorescence intensity was read to determine remaining adherent cells. For each well, adherent cell fraction was calculated as the ratio of postspin to prespin fluorescence readings.

Statistical Analyses. Nonlinear regression was used to fit experimental data to the appropriate model for radiolabeling, Ab affinity, and cell adhesion assays using SigmaPlot 5.0 (SPSS, Chicago, IL). Results for all experiments were analyzed by one-way ANOVA using SYSTAT 8.0 (SPSS). If treatments were determined to be significant, pairwise comparisons were performed using Tukey's post hoc test with a 95% confidence level considered significant.

Results

Model Surfaces and Protein. SAMs of alkanethiols on Au were selected to present a wide range of well-defined surface chemistries to examine the effects of surface chemistry on $FNIII_{7-10}$ adsorption. Long-chain functionally terminated alkanethiols ($HS-(CH_2)_n-X$, $n \geq 10$) adsorb from solution onto Au to form stable, well-packed and ordered monolayers.[34−36] The functional end groups (X) examined in this study were CH_3 (hydrophobic), OH (neutral hydrophilic), NH_2 (positively charged at physiological pH), and COOH (negatively charged at physiological pH). These SAM surfaces have been characterized by contact angle measurements as shown in Table 1 as well as by X-ray photoelectron spectroscopy (XPS).[29]

(31) Cutler, S. M.; Garcia, A. J. *Biomaterials* **2003**, *24*, 1759−1770.
(32) Garcia, A. J.; Ducheyne, P.; Boettiger, D. *J. Biomed. Mater. Res.* **1998**, *40*, 48−56.
(33) Reyes, C. D.; Garcia, A. J. *J. Biomed. Mater. Res.* **2003**, *65A*, 511−523.
(34) Porter, M. D.; Bright, T. B.; Allara, D. L.; Chidsey, C. E. D. *J. Am. Chem. Soc.* **1987**, *109*, 3559−3568.
(35) Ulman, A.; Eilers, J. E.; Tillman, N. *Langmuir* **1989**, *5*, 1147−1152.
(36) Bain, C. D.; Troughton, E. B.; Tao, Y. T.; Evall, J.; Whitesides, G. M.; Nuzzo, R. G. *J. Am. Chem. Soc.* **1989**, *111*, 321−335.

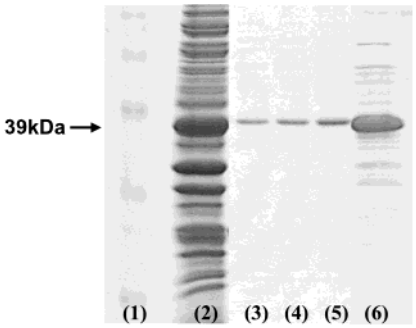

Figure 1. SDS-PAGE for purified $FNIII_{7-10}$ (39 kDa). Lane 1 is a molecular weight marker; lane 2 is lysate; lanes 3, 4, and 5 are sample fractions; and lane 6 is a concentrated sample.

Table 1. Contact Angle Measurements for SAMs (Mean ± Standard Error)

surface chemistry	contact angle (deg) mean (error)	surface chemistry	contact angle (deg) mean (error)
CH_3	107 (1)	COOH	28 (1)
OH	25 (3)	NH_2	43 (3)

$FNIII_{7-10}$ is a 39 kDa recombinant fragment of FN that encompasses the 7th through 10th type III repeats of the human pFN molecule.[37] $FNIII_{7-10}$ spans the central cell binding domain which includes the PHSRN synergy site in the 9th type III repeat of FN and the RGD binding motif in the 10th type III repeat. These motifs are required for binding of integrin $\alpha_5\beta_1$, a cellular receptor specific for FN.[38,39] The full pFN molecule is a large glycoprotein (440−480 kDa) that contains several functional domains other than cell binding, including sites for collagen and heparin binding as well as self-assembly.[40] We chose to use this recombinant fragment of FN to model full pFN in order to eliminate possible confounding effects from regions outside the central cell binding domain. Recombinant $FNIII_{7-10}$ was expressed and purified to high yields (Figure 1). Antibody and cell adhesion assays demonstrated equivalent functional activity between $FNIII_{7-10}$ and pFN (data not shown).

Kinetics of Protein Adsorption. Kinetics of $FNIII_{7-10}$ adsorption onto SAMs were determined by SPR. Kinetic profiles of fragment adsorption revealed an initial rapid association rate that then slowed with time and appeared to approach saturation (Figure 2). The saturating values varied among the surfaces, following the trend NH_2 > CH_3 > COOH = OH. On the CH_3 surface, the response overshoots at approximately 50% saturation and then climbs to a plateau suggesting that the protein adsorbs quickly and then goes through significant reorientation or conformational change. This overshoot observation is consistent with previous work.[41−43]

The adsorption process was analyzed using a mass action model with two states of the adsorbed protein: (1) reversibly adsorbed state and (2) irreversibly adsorbed state.[24,44,45] In the model, the protein first associates with the surface in a reversibly adsorbed state (Figure 3). A fraction of adsorbed molecules then undergo a structural/conformational change to an irreversibly adsorbed state. This model yields the following governing equations:

$$dY_1/dt = (kc - sY_1)(A_T(1 - fa_1Y_1 - fba_1Y_2)) - rY_1 \quad (1)$$

$$dY_2/dt = sY_1A_T(1 - fa_1Y_1 - fba_1Y_2) \quad (2)$$

$$Y_T = Y_1 + Y_2 \quad (3)$$

where Y_T is the total surface density of $FNIII_{7-10}$ on the surface (ng/cm^2), Y_1 represents the surface density of molecules adsorbed in state 1 (ng/cm^2), and Y_2 represents the represents the surface density of molecules adsorbed in state 2 (ng/cm^2). c is the concentration of molecules in solution (ng/cm^3), k represents the initial association rate of the protein (cm^{-1} s^{-1}), s represents the rate of conformational change from state 1 to 2 (cm^{-2} s^{-1}), and r represents the reversible rate of molecules in state 1 desorbed from the surface (s^{-1}). A_T is the total surface area (0.75 mm^2), a_1 represents the area occupied by one molecule in state 1 (cm^2/molecule × 10^{15}), b represents the ratio of the area occupied by a molecule in state 2 with respect to the area occupied by a molecule in state 1, and f is Avogadro's number divided by the molecular weight of the fragment (molecules/ng). The resulting SPR data is related to the total surface density of $FNIII_{7-10}$ such that it is the sum of the surface density of molecules in both states (eq 3).

Because the governing differential equations are nonlinear and an explicit solution is not available, the equations were solved numerically in conjunction with nonlinear regression analysis to yield kinetic parameters for each data curve. The regression results for Y_T, Y_1, and Y_2 on the four surface chemistries are shown in Figure 2, and the resulting kinetic parameters are listed in Table 2. The regression analysis yielded a χ^2 value for each curve fit such that $\alpha > 0.005$, and pairwise comparisons of model parameters yielded the following statistically significant results:

k: CH_3 > COOH = OH NH_2 > OH

s: OH > COOH

b: CH_3 > COOH = NH_2 = OH

r: CH_3 > COOH = NH_2 = OH

The modeling implemented here is based on the assumption that the protein adsorbs without mass transport limitations due to the flow of the protein through the flow cell. A calculation for mass transport limitation (MTL) of the system can be made using eq 4, where D is the diffusion coefficient (cm^2/s), F is the flow rate (μL/min), h and b are the dimensions of the flow cell (mm), and l_1 and l_2 are the detection points in the flow cell (mm).[46]

$$\mathrm{MTL} = \frac{L_r}{L_m + L_r} \qquad L_m = c_{L_m}\left[\frac{D^2F}{h^2bl_2}\right]$$

$$c_{L_m} = 1.47\frac{1 - (l_1/l_2)^{2/3}}{1 - (l_1/l_2)} \qquad L_r = kA_T \quad (4)$$

MTL varies from 0 when the system is not mass transport limited to 1 when the system is absolutely mass transport

(37) Leahy, D. J.; Aukhil, I.; Erickson, H. P. *Cell* **1996**, *84*, 155−164.
(38) Aota, S.; Nomizu, M.; Yamada, K. M. *J. Biol. Chem.* **1994**, *269*, 24756−24761.
(39) Garcia, A. J.; Schwarzbauer, J. E.; Boettiger, D. *Biochemistry* **2002**, *41*, 9063−9069.
(40) Hynes, R. O. *Fibronectins*; Springer-Verlag: New York, 1990.
(41) Soderquist, M. E.; Walton, A. G. *J. Colloid Interface Sci.* **1980**, *75*, 386−397.
(42) Lu, J. R.; Su, T. J.; Thirtle, P. N.; Thomas, R. K.; Rennie, A. R.; Cubitt, R. *J. Colloid Interface Sci.* **1998**, *206*, 212−223.
(43) Wertz, C. F.; Santore, M. M. *Langmuir* **2002**, *18*, 1190−1199.
(44) Lundstrom, I.; Elwing, H. *J. Theor. Biol.* **1984**, *110*, 195−204.
(45) Beissinger, R. L.; Leonard, E. F. *J. Colloid Interface Sci.* **1982**, *85*, 521−533.
(46) Christensen, L. L. *Anal. Biochem.* **1997**, *249*, 153−164.

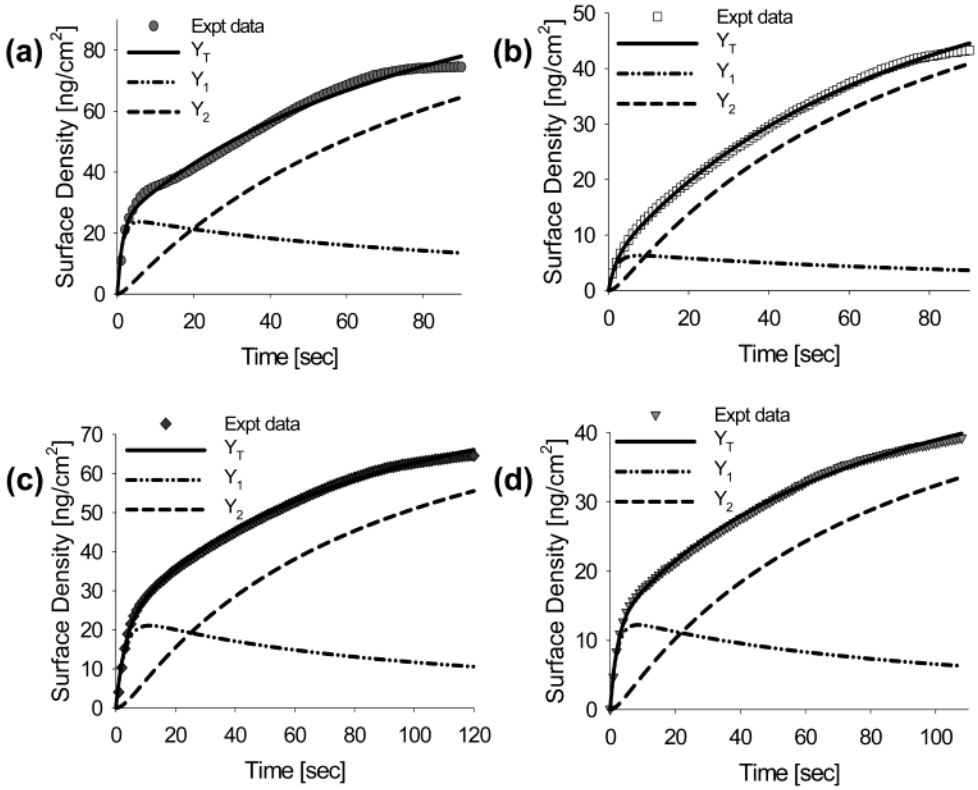

Figure 2. Representative kinetic model curve fits to SPR results: (a) CH_3, (b) OH, (c) NH_2, and (d) COOH. Y_1 is the amount of protein in state 1, Y_2 is the amount of protein in state 2, and Y_T is the total amount of $FNIII_{7-10}$ on the surface.

Table 2. Model Parameters Based on Fit to SPR Results (Mean ± Standard Error)

	k (cm^{-1} s^{-1}) mean (error)	s (cm^{-2} s^{-1}) mean (error)	$a_1 \times 10^{15}$ (cm^2/molecule) mean (error)	b (a_2/a_1) mean (error)	r (s^{-1}) mean (error)
CH_3	0.19 (0.014)	7.0 (1.0)	0.33 (0.026)	150 (5.0)	0.60 (0.036)
OH	0.049 (0.0030)	13 (1.3)	6.8 (0.32)	13 (0.64)	0.31 (0.018)
NH_2	0.14 (0.013)	7.3 (0.73)	2.4 (0.22)	28 (3.1)	0.32 (0.044)
COOH	0.080 (0.0041)	4.4 (0.48)	3.1 (0.23)	38 (3.4)	0.34 (0.019)
p	0.00096	0.041	0.000003	5.6×10^{-8}	0.025

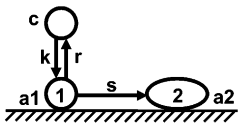

Figure 3. Protein adsorption model. k represents the initial association rate of the protein, s represents the rate of conformational change, a_1 represents the area occupied by the molecules in state 1, a_2 represents the area occupied by the molecules in state 2, and r represents the reversible rate of molecules leaving the surface from state 1.

limited. For the k values estimated in our analysis, the MTL index varies between 0.47 (OH) and 0.77 (CH_3). This range of MTL values indicates that the experiment is in the transitional regime from reaction rate limited to mass transport limited. Therefore, the fitted values for k underestimate the true association rate. However, these effective parameters still reveal surface-dependent differences.

Quasi-Equilibrium $FNIII_{7-10}$ Adsorption and Structure. $FNIII_{7-10}$ structural changes upon adsorption were evaluated as the adsorption process approached quasi-equilibrium. First, adsorbed $FNIII_{7-10}$ surface density was quantified as a function of coating concentration using radiolabeled protein. For each surface, adsorbed $FNIII_{7-10}$ density increased linearly until saturation values were approached at high concentrations (Figure 4). The adsorbed protein profiles of adsorbed FN (FN_{ads}) versus FN coating concentration ([FN]) were regressed to a simple

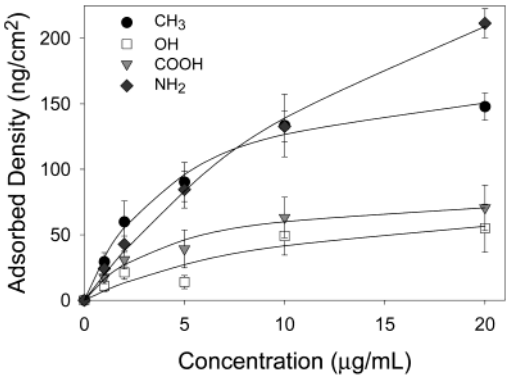

Figure 4. Adsorbed surface density of $FNIII_{7-10}$ on SAMs as a function of coating concentration.

hyperbola (eq 5) to obtain estimates of saturation density (FN_{sat}) and half-maximal adsorption ($[FN]_{50}$). $FNIII_{7-10}$ saturation density followed the trend $NH_2 > CH_3 > COOH = OH$. This trend in saturation density agrees well with our kinetic observations.

$$FN_{ads} = FN_{sat}\frac{[FN]}{([FN] + [FN]_{50})} \quad (5)$$

Conformational/structural changes were analyzed by ELISA with a panel of monoclonal Ab's. The use of

monoclonal antibodies as probes for structural or conformational changes in adsorbed proteins is well documented.[13,15,16,47,48] Adsorption of $FNIII_{7-10}$ onto synthetic surfaces is a relatively nonspecific process in which molecules are expected to be present in different orientations with respect to the surface. Only a portion of the adsorbed molecules are likely to display any particular domain in a position that is accessible to Ab binding. For molecules in which a particular binding domain is exposed, the average conformation of this domain is influenced by the chemical properties of the underlying surface. Three monoclonal Ab's directed against sites within the central integrin binding domain of FN were used to detect changes in conformation for both $FNIII_{7-10}$ and pFN. A sigmoidal binding curve (eq 6) was fit to Ab binding profiles of binding (AB_{bound}) versus adsorbed density (FN_{ads}) where AB_{bkgd} is the background Ab binding, AB_{sat} is the saturation level of Ab binding, AB_{50} is the half-maximal Ab binding, and b is the slope at the inflection point.

$$AB_{bound} = AB_{bkgd} + \frac{AB_{sat}}{1 + \exp\{-(FN_{ads} - AB_{50})/b\}} \quad (6)$$

Shifts in the Ab binding profiles (Figure 5), characterized by AB_{50}, reflect changes in Ab binding affinity for the protein adsorbed to the different surfaces. These changes in Ab binding affinity reflect adsorption-induced changes in protein conformation/structure and/or the prevention of Ab binding due to adsorbed orientation with respect to the surface. A right shift in the profile corresponds to a lower affinity of the Ab for that particular protein conformation because higher $FNIII_{7-10}$ densities are necessary to reach comparable amounts of Ab binding. Therefore, the AB_{50} parameter corresponds to the inverse of the Ab affinity. Similar shifts were detected for $FNIII_{7-10}$ and pFN (data not shown) using HFN7.1 and FNI-11, indicating that $FNIII_{7-10}$ is a useful model for the cell binding domain of pFN. Pairwise comparison analysis of HFN7.1 AB_{50} revealed statistically significant differences among surface chemistries ($p < 0.05$) such that HFN7.1 affinity followed the order $OH = NH_2 > COOH > CH_3$ (Table 3). Similarly, analysis of FNI-11 and mAB1937 AB_{50} demonstrated changes in Ab binding affinity in the order $OH = COOH = NH_2 > CH_3$.

FN tertiary structure consists of functional β-sheet folded globular domains connected by a flexible linker (Figure 6).[49] HFN7.1 binds to the flexible linker between the 9th and 10th type III repeats. The statistical trend for HFN7.1 binding suggests that the flexible linker undergoes significant structural changes upon adsorption of $FNIII_{7-10}$ with the OH SAM having the least amount of structural changes and CH_3 having the largest changes. The statistical trend for FNI-11 suggests that the 9th type III repeat undergoes structural changes on the CH_3 surface in comparison to the other three surfaces. Similarly, the loss in mAb1937 affinity for FNIII7−10 adsorbed onto CH_3 indicates considerable changes in the structure of the 8th type III repeat.

Cell Adhesion Centrifugation Assay. The activity of adsorbed $FNIII_{7-10}$ was investigated using a centrifugation adhesion assay that applies controlled, reproducible forces to adherent, fluorescently labeled cells. A sigmoidal adhesion curve was fit to the resulting adherent cell fraction (f) versus adsorbed fragment density (FN_{ads}) where f_{bkgd} is the background level of adhesion, f_{sat} is the maximum adhesion fraction, ADH_{50} is the half-maximal adhesion, and g is the slope at the inflection point.

$$f = f_{bkgd} + \frac{f_{sat}}{1 + \exp\{-(FN_{ads} + ADH_{50})/g\}} \quad (7)$$

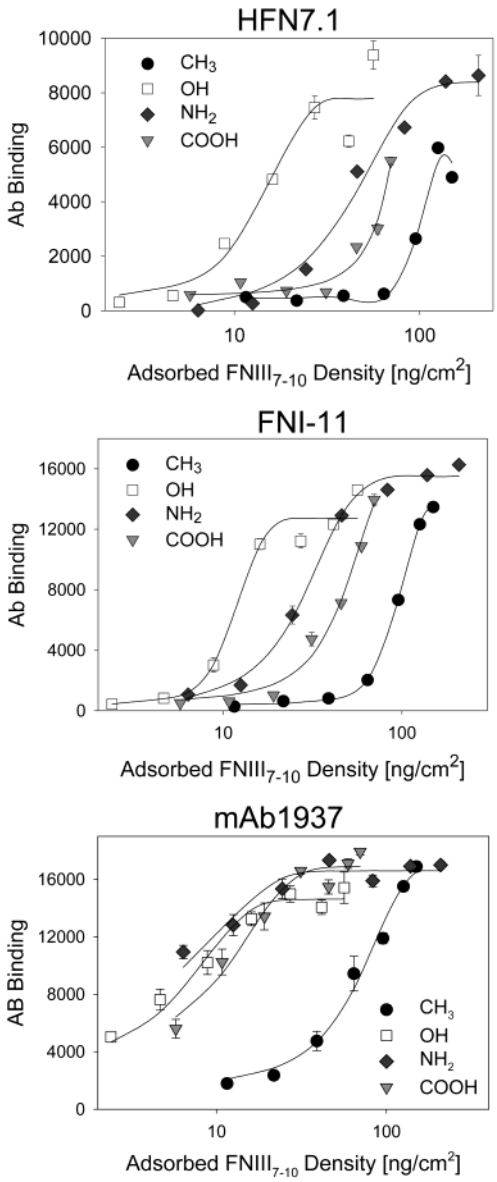

Figure 5. Ab binding affinity curves for HFN7.1, FNI-11, and mAb1937 Ab's. The concentration of $FNIII_{7-10}$ has been normalized by the surface density obtained by radiolabeling. Changes in Ab affinity, which reflect differences in protein conformation, are demonstrated as shifts in the normalized curves.

Table 3. Antibody-Based Assay for FN Conformation[a]

	HFN7.1 AB_{50} (error)	FNI-11 AB_{50} (error)	mAb1937 AB_{50} (error)
CH_3	160 (14)	74 (4.1)	59 (5.6)
OH	31 (2.2)	15 (1.2)	5.2 (0.79)
NH_2	62 (8.9)	22 (2.4)	4.2 (0.76)
COOH	92 (7.6)	35 (2.7)	8.2 (1.0)
p	0.0013	0.000029	0.00013

[a] AB_{50} represents the surface density of $FNIII_{7-10}$ required to reach 50% of the total Ab binding. This parameter is inversely proportional to Ab affinity (mean ± standard error).

(47) Ugarova, T. P.; Zamarron, C.; Veklich, Y.; Bowditch, R. D.; Ginsberg, M. H.; Weisel, J. W.; Plow, E. F. *Biochemistry* **1995**, *34*, 4457−4466.
(48) McClary, K. B.; Ugarova, T.; Grainger, D. W. *J. Biomed. Mater. Res.* **2000**, *50*, 428−439.
(49) Alexander, S. S., Jr.; Colonna, G.; Edelhoch, H. *J. Biol. Chem.* **1979**, *254*, 1501−1505.

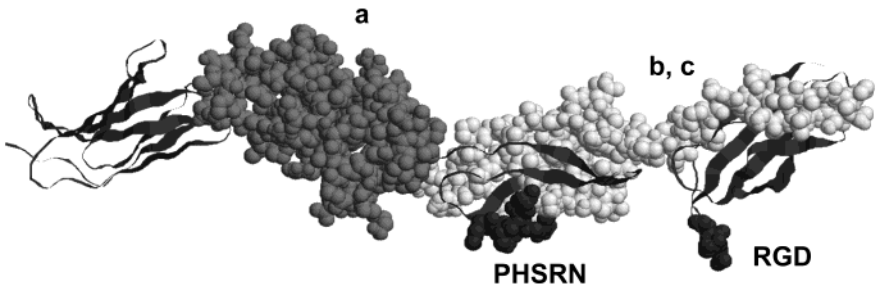

Figure 6. $FNIII_{7-10}$ model showing PHSRN and RGD binding sites and epitopes for (a) mAb1937, (b) FNI-11, and (c) HFN7.1.

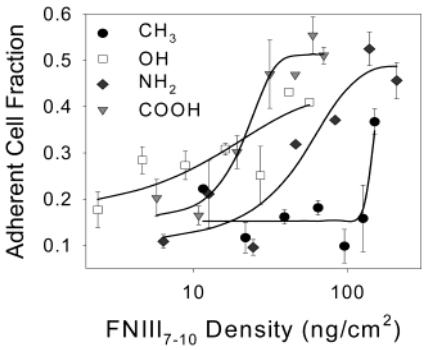

Figure 7. Cell adhesion strength to $FNIII_{7-10}$-coated SAMs. Shifts in adhesion profiles reflect differences in adhesion strength.

Changes in strength of cell adhesion to the various surfaces are shown in Figure 7 as shifts in the adhesion curve characterized by half-maximal adhesion (ADH_{50}). A shift in the curve to the right represents a decrease in adhesion strength since more protein is required on the surface for the adhesion of the cells to the substrate; therefore, adhesion strength is inversely related to ADH_{50}. Pairwise comparison testing of ADH_{50} among the SAMs revealed statistical differences that demonstrate changes in adhesion strength following the trend OH = NH_2 > COOH > CH_3 ($p = 0.00005$).

Structure/Function Relationships. To provide further insights into $FNIII_{7-10}$ adsorption, we examined correlations between the structural (AB_{50}) and functional (ADH_{50}) parameters. ADH_{50} correlated well with AB_{50} for HFN7.1 (linear, $R^2 = 0.98$) and FNI-11 (linear, $R^2 = 0.99$). This relationship indicates that structural alterations or adsorbed orientation effects in the 9th and 10th type III repeats of FN significantly modulate protein activity. In contrast, $FNIII_{7-10}$ adhesive activity correlated poorly with mAb1937 AB_{50}. This low correlation is expected because the epitope for this Ab lies outside the critical integrin binding region of $FNIII_{7-10}$. Finally, we examined the ability of surface hydrophobicity to predict adhesive activity. Contrary to previous reports,[24−28,50] surface hydrophobicity was a poor indicator of functional activity. These results indicate that surface hydrophobicity is not the primary parameter controlling adsorbed protein activity and that other surface properties, including charge, influence adsorbed protein function.

Discussion

We analyzed several adsorption parameters, including adsorption kinetics, quasi-equilibrium values, and structural changes (as determined by changes in Ab binding affinity), upon adsorption to well-defined surface chemistries for a FN model fragment. These parameters were correlated to the adhesive activity of the adsorbed protein in order to provide insights into adsorption−function relationships. The 30 min time point for cell adhesion to $FNIII_{7-10}$ was chosen to restrict interactions to initial adhesion events, ensuring that differences in adhesion could be attributed to FN conformation and thus eliminating confounding effects. Our group has shown that detachment of cells occurs at the integrin−FN bond for these cells.[51] In addition, blocking the integrin−FN interaction eliminates cell adhesion to these surfaces, confirming that our adhesion assay detects the functional activity of FN on each surface.[29]

Recent studies with model surfaces have proposed that surface hydrophobicity is a good predictor of adsorption parameters and that proteins adsorbed onto hydrophobic surfaces undergo greater unfolding/denaturation than on hydrophilic supports.[25−28,43,50] In agreement with these studies, our kinetic results indicate faster $FNIII_{7-10}$ adsorption rates for the CH_3 SAM and that proteins adsorbed onto this surface undergo that largest change in protein unfolding as determined by the ratio of area per molecule of irreversibly adsorbed protein (state 2) to area per molecule of reversibly adsorbed protein (state 1). Analysis of protein conformation using antibodies as structural probes revealed drastic reductions in Ab binding affinity for epitopes in the 8th, 9th, and 10th type III repeats of FN for proteins adsorbed onto the CH_3 functionality compared to other surfaces. These results suggest gross changes in FN structure throughout the entire molecule and agree well with the conclusions obtained from the kinetic analysis. Finally, $FNIII_{7-10}$ adsorbed onto the CH_3 SAM displayed poor cell adhesion activity. This loss in activity is in good agreement with the significant structural changes observed.

In contrast, kinetic parameters and surface hydrophobicity did not correlate well with FN activity on the OH, NH_2, and COOH surfaces. Similarly, no significant differences in the structure of the 8th type III repeat were detected among these surfaces using mAb1937. On the other hand, Ab measurements with two different Ab's revealed surface-dependent differences in the structure of the central cell binding domain of FN localized to the 9th and 10th type III repeats. These structural changes correlated well with surface-dependent differences in cell adhesive activity (Figure 8). $FNIII_{7-10}$ adsorption onto the neutral hydrophilic OH SAM exhibited the highest Ab binding affinity for Ab's localizing to the cell binding domain as well as the highest cell adhesion activity, suggesting that this functionality induces the least amount of protein unfolding or denaturation. The adsorption and functional behavior on the OH surface, as well as the

(50) Sigal, G. B.; Mrksich, M.; Whitesides, G. M. *J. Am. Chem. Soc.* **1998**, *120*, 3464−3473.

(51) Gallant, N. D.; Capadona, J. R.; Frazier, A. B.; Collard, D. M.; Garcia, A. J. *Langmuir* **2002**, *18*, 5579−5584.

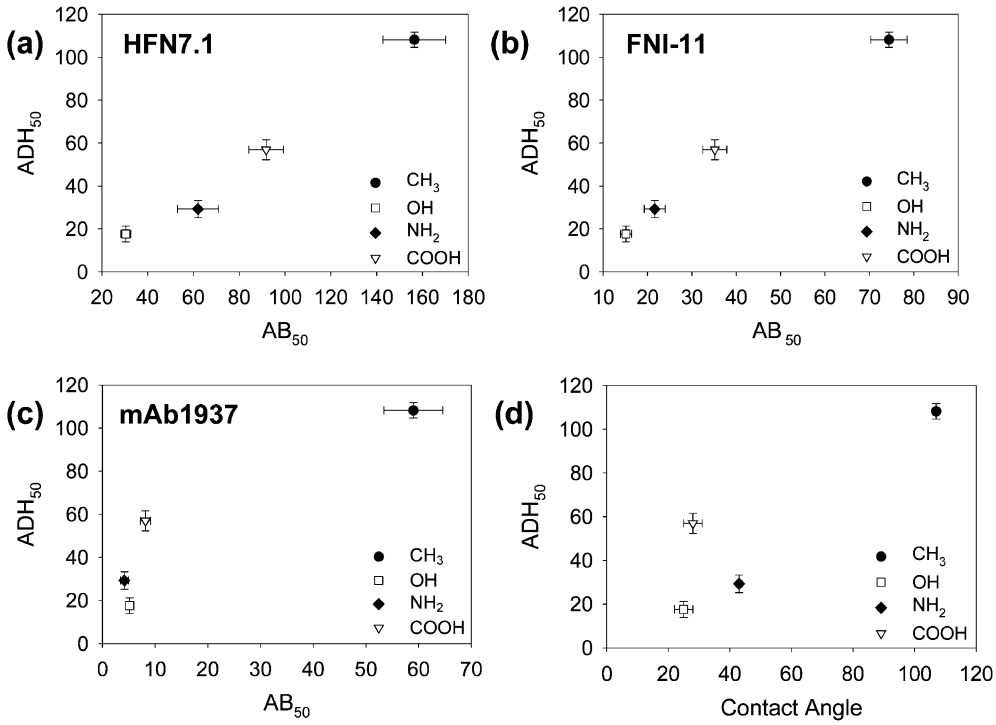

Figure 8. Structure−function relationships for adsorbed $FNIII_{7-10}$. Correlation of ADH_{50} with (a) HFN7.1 (linear, $R^2 = 0.98$), (b) FNI-11 (linear, $R^2 = 0.99$), (c) mAB1937, and (d) contact angle.

hydrophobic CH_3, may be explained by water solvation and restructuring effects at the interface.[52,53]

This analysis indicates that surface hydrophobicity and adsorption kinetic parameters are partial predictors of adsorbed FN functional activity when comparing hydrophobic and hydrophilic supports. These determinants are likely to be effective for gross/global changes in protein structure. However, these parameters cannot discriminate among neutral, positive, and negative hydrophilic surfaces, even though adsorption onto these functionalities significantly modulates the activity of the adsorbed protein. In contrast, probes for specific structural/functional domains, such as the Ab's used in the present study, provide robust determinants of adsorbed FN activity. Furthermore, the Ab-specific differences among SAMs indicate that local, indicated by each individual Ab, as well as global, indicated by combining the results of all three Ab's, changes in protein structure potentiate protein activity. While the present study provides insights into adsorption-induced changes in structure and function, detailed structure−function analyses are required to elucidate mechanisms involved in surface-dependent modulation of protein activity. As an initial step to this goal, we recently implemented computational molecular modeling approaches to the adsorption of the FN fragment onto the SAMs examined in the present work.[54] This computational molecular model predicted adsorption free energy following the trend $NH_2 > CH_3 > COOH > OH$ and structural changes following the trend $CH_3 > COOH = NH_2 > OH$, both of which are consistent with the experimental results obtained in the present study. Finally, similar structure−function analyses with other proteins are necessary to establish the broad applicability of this approach to analyze protein adsorption to synthetic supports.

Conclusions

Using model surfaces with well-defined surface properties and investigating a range of surface chemistry, we demonstrate significant surface-chemistry-dependent structural changes in FN central cell binding domains and adhesive activity. These findings indicate that adsorption-induced changes in protein structure and activity are not dominated by surface hydrophobicity alone. This study also establishes a relationship between surface-dependent changes in structural domains of FN and FN functional activity.

Acknowledgment. This work was supported by a National Science Foundation (NSF) grant (BES-9986549), the Georgia Tech/Emory ERC on the Engineering of Living Tissues (EEC-9731643), and a NSF graduate fellowship awarded to Kristin Michael. Transformed bacteria were kindly provided by H. P. Erickson (Duke University). FNI-11 was kindly provided by M.H. Ginsberg (Scripps Research Inst.). HFN7.1 monoclonal antibody was obtained from the Developmental Studies Hybridoma Bank developed under the auspices of the NICHD and maintained by the University of Iowa, Department of Biological Sciences, Iowa City, IA 52242.

LA034810A

(52) Basalyga, D. M.; Latour, R. A., Jr. *J. Biomed. Mater. Res.* **2003**, *64*, 120−130.

(53) Latour, R., Jr.; Rini, C. J. *J. Biomed. Mater. Res.* **2002**, *60*, 564−577.

(54) Wilson, K.; Stuart, S. J.; Garcia, A. J.; Latour, R. A., Jr. *J. Biomed. Mater. Res.*, submitted.